FPGA Implementation and Experimental Performances of a novel Timing Synchronization Method in MIMO-OFDM Systems

En Zhou, Xiaolin Hou, Jianping Chen, Zhan Zhang, and Hidetoshi Kayama
Innovative Radio Transmission Lab, DoCoMo Beijing Communication Laboratories Co., Ltd
Beijing P.R. China
Email: {zhou, hou, j.chen, z.zhan, kayama}@docomolabs-beijing.com.cn

***Abstract*—This paper proposes a novel preamble structure and a timing synchronization method for OFDM systems. The preamble structure has both properties of delayed and symmetric correlations which can afford accurate time and frequency synchronization simultaneously. A new timing metric is also proposed according to the preamble structure, which is the production of the modulus of delayed and symmetric correlation profiles. The proposed algorithm has been implemented with FPGA in MIMO-OFDM testbed. The measured timing performances are well accordance with the simulation results. The timing performance is very accurate when SNR is larger than 5dB, that the probability of timing shift compared to the first path less than 10 samples is above 99.5% in 3GPP Case 2 channel. And the timing shifts only distribute on several discrete positions. Furthermore, the timing synchronization can work well in high mobility environment up to 500km/h.**

I. Introduction

Orthogonal Frequency Division Multiplexing (OFDM) is an effective technique to combat multipath fading. Multiple Input Multiple Output (MIMO) technique can well improve transmission quality or increase system capacity. OFDM and MIMO have been the core technologies for future broadband wireless communications.

Synchronization is important for OFDM systems. Till now, a lot of methods [1]-[8] have been proposed, in which large amount of methods are based on preambles. Such preamble based methods have satisfied and robust synchronization performances with low computational complexity. Generally, they can be further divided into two categories: delayed correlation based methods [1]-[2] and symmetric correlation based methods [3]-[5][8]. The principal merit of delayed correlation based methods is that it is easy for real implementation and can perform time and frequency synchronization simultaneously. However, the obtained timing metric is triangle-like shape, which is hard to get accurate timing performances. As to the symmetric correlation based methods, the principal merit is that it can obtain pulse-like timing metrics, which is advantageous for accurate timing performances. However, the computational complexity is much larger. We have proposed a new preamble structure and synchronization method which have combined the merits of delayed correlation based methods and symmetric correlation based methods [9]. And this method will be further implemented using Field Programable Gate Array (FPGA) with some modifications in our MIMO-OFDM testbed to further verify its feasibility and superiority.

The rest of the paper is organized as follows: The proposed preamble structure and timing metric is simply introduced in Section II. The experimental setup and hardware implementation is described in Section III and Section IV respectively. The performances comparison is discussed in Section V. Finally, Section VI gives the conclusion.

II. Proposed Preamble Structure and Timing Metric

The proposed synchronization preamble structure is shown in Fig. 1. The whole preamble is divided into four parts, serially denoted as $\mathbf{C}$, $\mathbf{D}$, $\mathbf{C}$, $\mathbf{D}$. Sequence $\mathbf{D}$ is the rotated reversed and conjugated version of sequence $\mathbf{C}$. If sequence $\mathbf{C}$ is defined as $\mathbf{C} = \{x(m)\}_{m=0}^{M-1}$, the corresponding sequence $\mathbf{D}$ can be expressed as $\{\exp(j\varphi)x^*(M-m)\}_{m=0}^{M-1}$, where φ is a common phase, and $x(M) = x(0)$. Thus $\mathbf{D} = \exp(j\varphi)(\overleftarrow{\mathbf{C}})^*$, in which superscript $\leftarrow$ and * represent reverse operation and conjugate operation respectively. Pair $\{\mathbf{C}, \mathbf{D}\}$ is called one basic element with length of $2M$, as shown in Fig. 1. The preamble structure is just the two repetition version of basic element. If M/N is equal to $1/4$ or $1/2$, where N is the length of OFDM symbol, the preamble can be obtained directly by transforming a rotated real sequence using IFFT operation [9]. Hence, the preamble structure is flexible for construction and virtual subcarrier friendly. And the preamble structure has delayed and symmetric correlation properties, accurate timing and frequency synchronization can be performed simultaneously. Using the delayed correlation property, conventional Moose scheme can be used for frequency offset estimation [1]. In this paper, only timing synchronization will be discussed by using the preamble structure.

Step 1: The delayed correlation based timing metric is defined as

$$M_d(k) = \frac{|\Gamma_d(k)|^2}{P(k) \cdot P(N_d + k)} \tag{1}$$

where, Γ_d is the delayed correlation profile and can be calculated as $\Gamma_d(k) = \sum_{m=0}^{2M-1} r^*(k+m)r(k+N_d+m)$; P is the received signal power and can be calculated as $P(k) = \sum_{m=0}^{2M-1} |r(k+m)|^2$. $r(n)$ is the received signal. M is

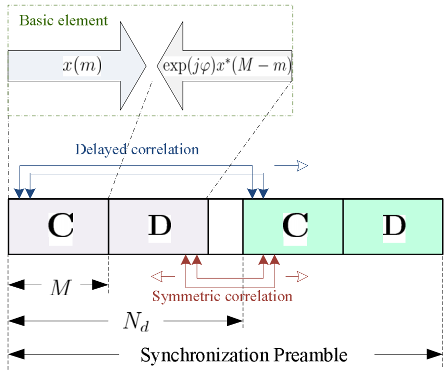

Fig. 1. Proposed preamble structure

the half length of basic element and N_d is the distance between two basic elements in the preamble as shown in Fig. 1.

Step 2: The final timing metric is defined as

$$M(k) = M_d(k) \cdot |\Gamma_s(k)|^2 \quad (2)$$

where Γ_s is the symmetric correlation profile and can be calculated as $\Gamma_s(k) = \sum_{m=0}^{2M-1} r(k+2M-m)r(k+N_d+m+1)$.

III. Experimental Setup

We are focusing on experimental burst packet signal transmission using MIMO-OFDM radio access. 3GPP Case 2 channel model [10] will be employed in our investigation and experimental channel emulation. The major system parameters are listed in Table I.

The schematic diagram of the implemented MIMO-OFDM transmitter and receiver are shown in Fig. 2. At transmitter side, the serial binary information data bits are serial-to-parallel (S\P) converted to four streams corresponding to each transmitter antenna branch. In each antenna branch, the binary information is turbo coded and modulated by 16QAM. The modulated signal is mapped into the 896 data subcarriers and converted into time domain signals by IFFT operation. After appending the guard interval, the time domain data signal is reshaped according to the frame structure and multiplexed with the preamble signals in time domain. After filtering and digital-to-analog conversion (DAC), the analog signal is up-converted into the Radio Frequency (RF) signal and then passed to the channel emulator to emulate the MIMO channel effect. At receiver side, the received RF signal is first down-converted, analog-to-digital conversion (ADC) and filtering. Then, timing synchronization is performed to find the frame start position and the corresponding FFT window position of each OFDM symbol. And then, frequency offset estimation and compensation is operated for each receive antenna signal. After removing of the guard interval, FFT is used to convert the obtained signal into frequency domain. Then, channel estimation and MIMO detection is performed. Finally, the soft bit information is calculated for Turbo de-coder. The decoded bits stream for each transmitter antenna branch is subjected to parallel-to-serial (P\S) conversion to regenerate the transmitted information stream.

TABLE I
Parameters of the Experimental System

System	MIMO-OFDM
Carrier frequency	2.5GHz
Bandwidth	12.5MHz
Subcarrier separation	12.2kHz
FFT size	1024
CP length	7.68μs (96 samples)
Number of data subcarriers	896
Number of symbols per frame	32
Number of synchronization preambles per frame	2
Number of transmit / receive antennas	4×4
Modulation level for data symbols	16QAM
Format of fixed-point signal in implementation	Fix_16_12
Channel Model	3GPP Case 2

Synchronization is important for the whole system. In our experimental MIMO setup, the time delays between different transmit/receive antenna pairs are much small compared to the channel delay. Hence, MIMO channel can be regarded as a whole for timing synchronization. Furthermore, the transmit antennas are well synchronized by equipment. At receiver, there may be exist some frequency offsets among the signals from different receive antennas. So, frequency offset estimation and compensation should be performed for each receive antenna, as illustrated in Fig. 2. At transmitter, only one of the four transmit antennas transmits the synchronization preamble. This is because that the timing performance is mainly related to the received SNR. Only if the total preamble energy is the same, the timing performances would be the same whatever it is assigned on one transmit antenna or four transmit antennas. In our experimental MIMO testbed, the synchronization preamble is constituted of two CP appended OFDM symbols. Hence, M and N_d in the above equations is equal to $N/2$ and $N+G$ respectively, where N is the OFDM symbol length and G is the cyclic prefix length.

IV. Hardware Implementation

For FPGA implementation, symmetric correlation is a computational burden. A large number of multipliers and adders are needed and operate parallel which will cost a large amount of FPGA resource, especially when the preamble length is long. In order to greatly reduce the computational complexity of symmetric correlation and also the hardware resource, two bits three states quantification of [-1, 0 +1] is adopted. And the timing performance would not be reduced much. For convenience of hardware realization, the timing metric is better not normalized. The timing detection threshold should be designed having abilities of not only tracking the channel variety but also avoiding the effect of side peaks.

Fig. 3 shows the flow chart of the timing synchronization implementation. The received signal of one receive antenna would pass through four channels in parallel. The first channel is to calculate the symmetric correlation profile. Before calculation of the symmetric correlation, the signal is first quantified

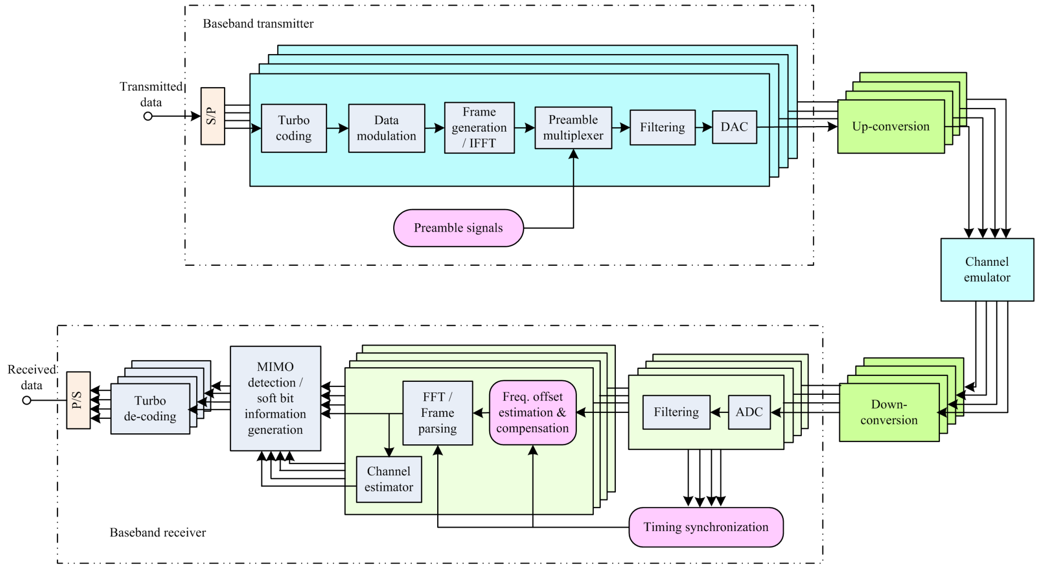

Fig. 2. Schematic diagram of the experimental MIMO-OFDM system

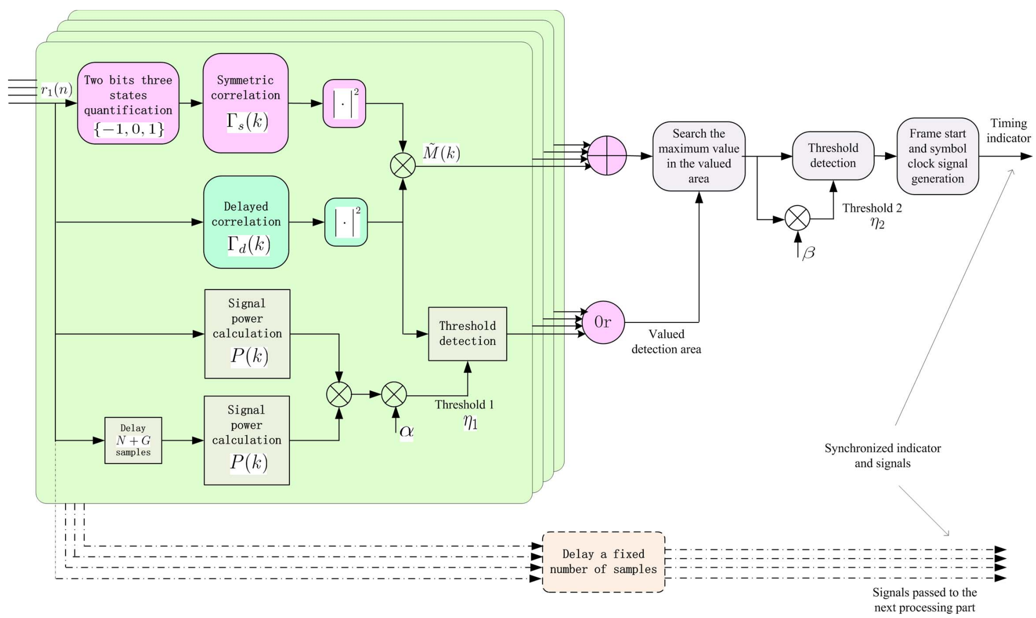

Fig. 3. Flow chart for the timing synchronization implementation

into two bits with three states [-1, 0, 1] according to a proper noise threshold. Then symmetric correlation operation is performed to generate the symmetric correlation profile, $\Gamma_s(k)$. The second channel is to calculate the delayed correlation profile $\Gamma_d(k)$. The third channel is to calculated the received signal power $P(k)$ and the fourth is to calculate the delayed signal power $P(N_d+k)$. Threshold 1 is obtained according to the received signal power, $\eta_1 = \alpha \cdot P(k)P(N_d+k), \alpha \in (0,1)$. According to the modulus of delayed correlation profile, $|\Gamma_d(k)|^2$, the valued detection area Ω can be founded, that $\Omega = \{k \,|\, |\Gamma_d(k)|^2 > \eta_1\}$. The final timing metric is obtained by multiplying the modulus of symmetric correlation profile and delayed correlation profile, $\tilde{M}(k) = |\Gamma_s(k)|^2 \cdot |\Gamma_d(k)|^2$. Then the maximum value of $\tilde{M}(k)$ in the valued detection area is searched, denoted as $\tilde{M}_{max} = \max\{\tilde{M}(k)\}_{k\in\Omega}$. Threshold 2 is obtained by scaling the maximum value with a factor β, $\eta_2 = \beta \cdot \tilde{M}_{max}, \beta \in (0,1)$. The first position of the delayed timing metric larger than threshold 2 would be decided as the desired position of the first path, which would give a pulse to trigger the following function block to generate the frame start indicator and OFDM symbol clock signals. If using the signals of multiple receive antennas in timing synchronization to further improve the performance, the timing metric of each antenna should be added and the valued detection areas should be combined before searching the maximum value of the final timing metric, as shown in the Fig. 3. The original received

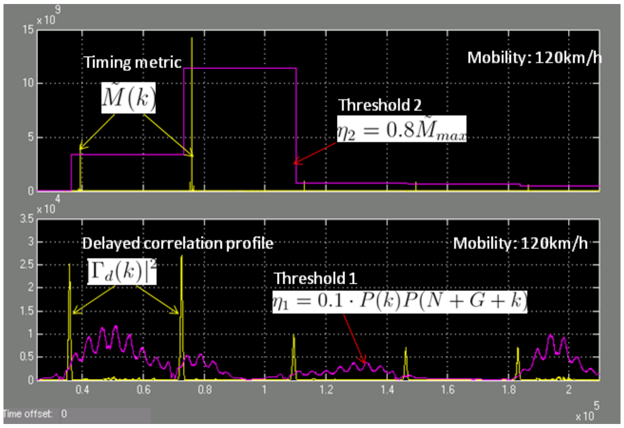

Fig. 4. Example of threshold 1 ($\alpha = 0.1$) and threshold 2 ($\beta = 0.8$)

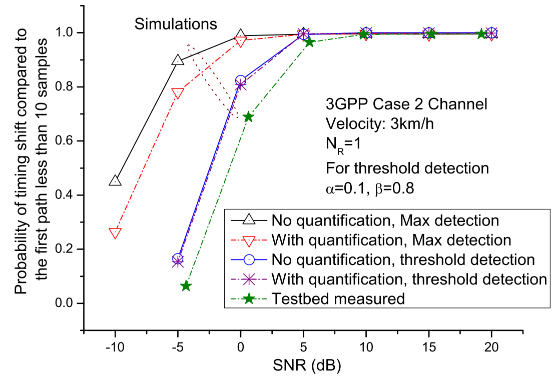

Fig. 5. Timing performance with the SNR

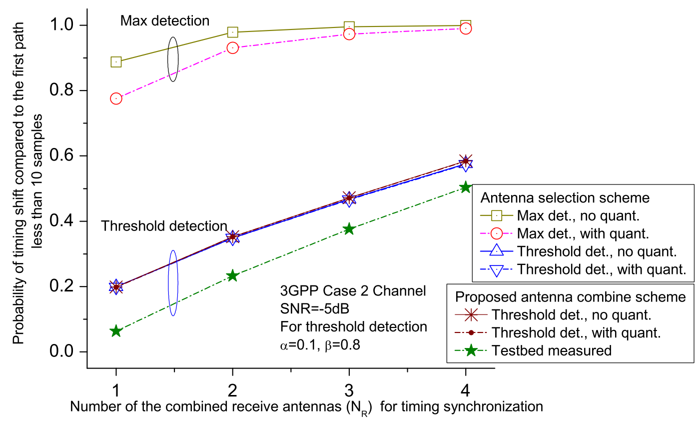

Fig. 6. Timing performance with the number of receive antennas

signal would be delayed a fixed number of samples time to be synchronized with the generated indicator.

Fig. 4 gives an example of the two thresholds which is captured from testbed. The bottom sub-figure is the delayed correlation profile and threshold 1, which varies very large with the signal power in high mobility environment. The normalized correlation profile by signal power will be much static. Thus, driver is needed for normalization operation, which is challenging for hardware implementation. In our testbed, threshold 1 is the scaled signal power, which can avoid the driving operation and make the hardware implementation more easy. The scale factor α would affect the detection performance and the threshold SNR for correct detection. The top subfigure is an example of the final timing metric and threshold 2. According to the obtained detection area, the maximum value of the timing metric in the detection area is searched and scaled with a factor β as threshold 2. Threshold 2 is obtained according to the current timing metric. So, it would not result frame detection lost.

V. Laboratory Experimental Results

Fig. 5 gives the timing performance as a function of SNR in low mobility environment, in which $N_R = 1$ means that only one receive antenna signal takes part in timing synchronization. Maximum detection is that timing decision is obtained by searching the position with the maximum value of the final time metric. As shown in Fig. 5, the maximum detection has the best timing performance, which is the theoretical upper bound. Threshold detection has a performance loss in low SNR environment. As for two bits three states quantification for symmetric correlation, it would bring a little performance loss in low SNR environment when using maximum detection. While for threshold detection, the quantification would not degrade the timing performance. When SNR is large than 5dB, the timing performance are very well and almost the same whatever using maximum detection or threshold detection and whatever with or without quantification. Because threshold detection is practical for real implementation, quantification would not degrade the real timing performance. And there is a threshold SNR for threshold detection. Scale factor α would affect the detection threshold. Small value of α would lead to low threshold and get better performance in low SNR environment while the error detection would increase in high SNR environment, vice versa. To guarantee the timing performance in high SNR environment, a middle value 0.1 is selected for scale factor α. The line marked with five pointed start is the measured results in our testbed. We can see that there is a little performance loss when SNR is less than 5dB, and the performances are almost the same when SNR is larger than 5dB. Considering the difference of measured SNR and the accuracy loss for fixed number of bits in hardware implementation, the measured timing performances are well accordance with the simulation results.

As shown in Fig. 5, the timing performance is accurate enough when SNR is larger than 5dB even only using one receive antenna signal. There is no gap to further improve its performance by using multiple antennas' signals in high SNR environment. In low SNR environment, the timing performance has potential to be improved by combination of multiple antennas' signals. Fig. 6 plots the timing performance as a

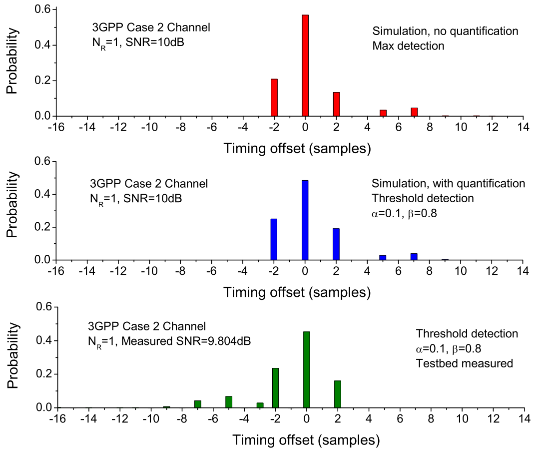

Fig. 7. PDF performance comparison

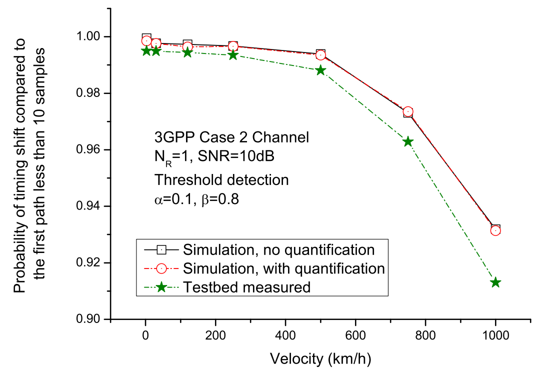

Fig. 8. Timing performance with mobility

function of the number of receive antennas for combination in timing synchronization when SNR is equal to -5dB. Antenna selection algorithm is selected as a reference for its good performance, that the antenna signal with the largest receive power will be selected to perform timing synchronization. From Fig. 6, we can see that the timing performances would be improved with the increase of the number of received antennas whatever using maximum detection or threshold detection. However, antenna selection is not feasible for real implementation because it is hard to control the switch time and guarantee an integrated synchronization preamble signal at the same time. And the proposed method, as shown in Fig. 3, is feasible in real application and can reach the same performance of the ideal antennal selection algorithm. The testbed measured result has the same trend with but a little worse than that of simulations.

Fig. 7 is the probability density function (PDF) performance comparison among simulation results of maximum detection with no quantification, simulation results of threshold detection with quantification and testbed measured results when SNR=10dB. We can see that, the timing performances are very accurate and the timing shifts are only distributed on several discrete positions, which has relations with the multipath channel model. And the ranges of timing shift are about 10 samples, which is very small and the CP length can be shortened improving the spectrum efficiency.

Fig. 8 gives the timing performance as a function of mobility when using threshold detection. With the increase of mobility, the timing performances would be slightly degraded whatever by simulations or testbed measured. And the testbed measured timing performance is a little worse than that of simulations. When the mobility is less than 500km/h, the probability of timing shift compared to the fist path less than 10 samples is larger than 99%. It is accurate enough for real application. So, we can say that our designed and implemented timing synchronization algorithm can work well in high mobility environment up to 500km/h.

VI. Conclusion

In this paper, a novel preamble structure and synchronization method has been proposed, which combines the merits of symmetric and delayed correlation based methods. The preamble structure can be easily constructed in frequency domain and is also spectrum efficient. The proposed algorithm has been implemented with FPGA in our MIMO-OFDM testbed. The measured timing performances are well accordance with the simulation results. The timing performance is accurate enough for real application when SNR is larger than 5dB, that the probability of timing shift compared to the first path less than 10 samples is above 99.5% in 3GPP case 2 channel. And the timing shifts only distribute on several discrete positions which has relations with the channel model. Furthermore, the timing synchronization can work well in high mobility environment up to 500km/h.

References

[1] P.H. Moose, "A technique for orthogonal frequency-division multiplexing frequency offset correction," *IEEE Trans. on Commu.*, vol.42, no.10, pp.2908-2914, Oct. 1994.
[2] T.M Schmidl, D.C. Cox, "Robust frequency and timing synchronization for OFDM," *IEEE Trans. on Commu.*, vol.45, pp.1613- 1621, Dec. 1997.
[3] B. Park, H. Cheon, and D. Hong, "A novel timing estimation method for OFDM systems", *IEEE commun. letters*, vol.7, no.5, pp. 239-241, May 2003.
[4] K.C. Kim, "Method for creating symmetric-identical preamble and method for synchronization symbol and frequency of orthogonal frequency division multiplexed signals by using symmetric-identical preamble", *SAMSUNG ELECTRONICS CO., LTD.*, *US patent*, Pub. No.: US 2003/0072256 A1, Pub. Date: Apr. 17, 2003.
[5] M. Morelli, "Timing and frequency synchronization for the uplink of an OFDMA system," *IEEE Trans. on Commu.*, pp.296-306, Feb. 2004.
[6] E. Zhou, X. Zhang, and W.B. Wang, "Synchronization algorithms for MIMO OFDM systems," *IEEE WCNC 2005*, pp.18-22, March 2005.
[7] E. Zhou, Y.Y. Yan, and W.B. Wang, "A Novel Timing Synchronization Method for Localized OFDMA Uplink System," *IEEE ICC 2006*, vol.11, pp.5086-5090, June 2006.
[8] Z.S. Zhang, H. Kayama, and C. Tellambura, "Joint Frame Synchronization and Carrier Frequency Offset Estimation in Multicarrier Systems," *IEEE GLOBECOM 2006*, pp.1-6, Nov. 2006.
[9] E. Zhou, X.L. Hou, Z. Zhang and H. Kayama, "A Preamble Structure and Synchronization Method based on Central-Symmetric Sequence for OFDM Systems," *IEEE VTC 2008 Spring*, May 2008.
[10] 3GPP, TR 25.996, http://www.3gpp.org/ftp/Specs/html-info/25996.htm